Periodico di Mineralogia (2011), 80, 1 (Special Issue), 39-55 DOI: 10.2451/2011PM0004

PERIODICO di MINERALOGIA
established in 1930

An International Journal of
MINERALOGY, CRYSTALLOGRAPHY, GEOCHEMISTRY, ORE DEPOSITS, PETROLOGY, VOLCANOLOGY
and applied topics on *Environment*, *Archeometry* and *Cultural Heritage*

Special Issue in memory of Sergio Lucchesi

Synthesis and Mössbauer characterization of $Fe_{1+x}Cr_{2-x}O_4$ ($0 \leq x \leq 2/3$) spinel single crystals

Marco Quintiliani[1], Giovanni B. Andreozzi[1,*] and Henrik Skogby[2]

[1]Dipartimento di Scienze della Terra, Sapienza Università di Roma, Italy
[2]Department of Mineralogy, Swedish Museum of Natural History, Stockholm, Sweden
[*]Corresponding author: *gianni.andreozzi@uniroma1.it*

Abstract

Spinel single crystals belonging to the $FeCr_2O_4$-Fe_3O_4 join were synthesized by a flux growth method ($Na_2B_4O_7$ as flux, temperature range of 1200-900 °C and cooling rate of 4 °C/h). Crystals with compositions corresponding to $Fe_{1+x}Cr_{2-x}O_4$ ($0 \leq x \leq 2/3$) were obtained and successively investigated by a combined microchemical, diffractometric and spectroscopic approach.

Fe-Cr-spinel single crystals produced are of different quality (in terms of size and shape). The flux content in the starting mixture showed to have the most relevant influence on the quality of synthetic products. Electron microprobe analysis evidenced a chemical heterogeneity for crystals of the same batch, with small crystals (down to 50 μm) being more homogeneous than the large ones. Mössbauer spectroscopy was used to determine the actual Fe^{3+}/Fe_{tot} ratios and highlighted the absence of magnetic phases.

The combined chemical and spectroscopic approach allowed to exclude any deviation from stoichiometry due to oxidation. In contrast with most of the existing literature, Mössbauer spectroscopy indicated the $Fe^{2.5+}$ valence state to be present even for iron poor samples with composition close to the end member chromite.

Key words: chromite-magnetite solid solution; synthesis, spinel single crystals; Mössbauer spectroscopy.

Introduction

Spinels belonging to the chromite-magnetite series are generally associated with upper-mantle-derived rocks, such as peridotites and serpentinites. They often occur in ophiolitic sequences and are valuable petrogenetic indicators of the environment of formation due to the cation arrangement and the iron valence states (Sack, 1982; Dick and Bullen, 1984). Several geothermobarometric models involving spinel phase equilibria have been proposed for

the estimation of upper mantle intensive parameters such as temperature and oxygen fugacity (Roeder et al., 1979; Fabriès, 1979; O'Neill and Wall, 1987; Ballhaus et al., 1991). In addition, Fe-Cr-spinels are studied in Materials and Solid State Sciences, because their composition and site distribution have strong effects on magnetic, electrical and thermo-chemical properties (Shukla et al., 1999; Fierro et al., 2005; Yunus et al., 2008).

The AB_2O_4 double oxides with $Fd\bar{3}m$ symmetry (spinels sensu lato) are based on a structure made of a densely-packed oxygen array with A and B cations of variable valence in tetrahedral (T) and octahedral (M) coordination. Geometrical constraints imposed by symmetry result in a rigid arrangement with the oxygen fractional coordinates (u, u, u) as the only independent variable. Every tetrahedron is surrounded by 12 octahedra, and every octahedron is surrounded by 6 octahedra and 6 tetrahedra. Cation distribution is described by the general formula $^{T}(A_{1-i}B_i)^{M}(A_iB_{2-i})O_4$, where i accounts for cation disorder and is commonly indicated as inversion parameter. There are two completely ordered configurations: normal ($i = 0$) and inverse ($i = 1$). Disorder takes place at increasing temperature, since A and B cations undergo increasing intersite exchange over T and M cationic sites, and i tends to the limit value of 2/3.

The chromite-magnetite solid solution, $Fe_{1+x}Cr_{2-x}O_4$ with x representing Fe^{3+} (Robbins et al., 1971) is particularly complex, as evidenced by the non-linear variation of unit cell parameter with composition (Figure 1). On the basis of experimental data and thermodynamic models three distinct regions were observed (Yearian et al., 1954; Francombe, 1957; Robbins et al., 1971; Levinstein et al., 1972; Wasilewski et al., 1975; Gillot et al., 1976; Ziemniak and Castelli, 2003). Latter authors, in particular, divided the $Fe_{1+x}Cr_{2-x}O_4$ binary solid solution in three distinct regions: I ($0 \geq x \geq 2/3$); II ($2/3 \geq x \geq 4/3$) and III ($4/3 \geq x \geq 2$). These authors considered analysis of the chromite-rich region I as the most straightforward since Fe^{3+} ions would be present only on octahedral sites partly substituting Cr (confined into M site due to its very high octahedral coordination preference). Accordingly, the cation distribution pattern may be written as $^{T}(Fe^{2+})^{M}(Cr_{2-x}\ Fe^{3+}{}_x)O_4$. In region III, on the contrary, Fe^{3+} fully substitutes Cr and, under the hypothesis of equal distribution between tetrahedral and octahedral coordination, the cation distribution may be written as $^{T}(Fe^{2+}{}_{1-x/2}\ Fe^{3+}{}_{x/2})^{M}(Cr_{2-x}\ Fe^{2+}{}_{x/2}\ Fe^{3+}{}_{x/2})O_4$. A rapid electron exchange reaction (hopping) occurs between adjacent, octahedrally coordinated Fe^{2+} and Fe^{3+} ions in magnetite ($x = 2$) so that the two ions become (nearly) indistinguishable (Verwey et al., 1947; Daniels and Rosencwaig, 1969). The electron hopping phenomenon is predicted by Ziemniak and Castelli (2003) to take place when equal amounts of Fe^{2+} and Fe^{3+} ions occupy the octahedra, that is, such behavior requires that electron hopping occurs in a pair-wise manner. In region II the electron pair-hopping concept is still retained, but excess Fe^{3+} ions on octahedra are expected to be distinguishable because it is no longer possible to retain equal amounts of Fe^{3+} and Fe^{2+} ions on octahedra. In any case, the quantification of this process is a problem not solved yet.

Because of the chemical complexity frequently observed in natural spinels and the difficulties in accurate site assignment of the major cations, synthetic materials of well-known compositions are generally studied to minimize system complexity. Most of the studies on Fe-Cr-spinels are based on synthetic powder samples, but they are often in disagreement regarding cation distribution (e.g., Yearian et al., 1954; Francombe, 1957; Derbyshire and Yearian, 1958; Levinstein et al., 1972; Ok et al., 1978; Petric and Jacob, 1982; Kose and Lida, 1984; Ishikawa et al., 1999; Viart et al., 2000; Barrero et al., 2001). A possible explanation is the difficulty of crystal chemical characterization of powder

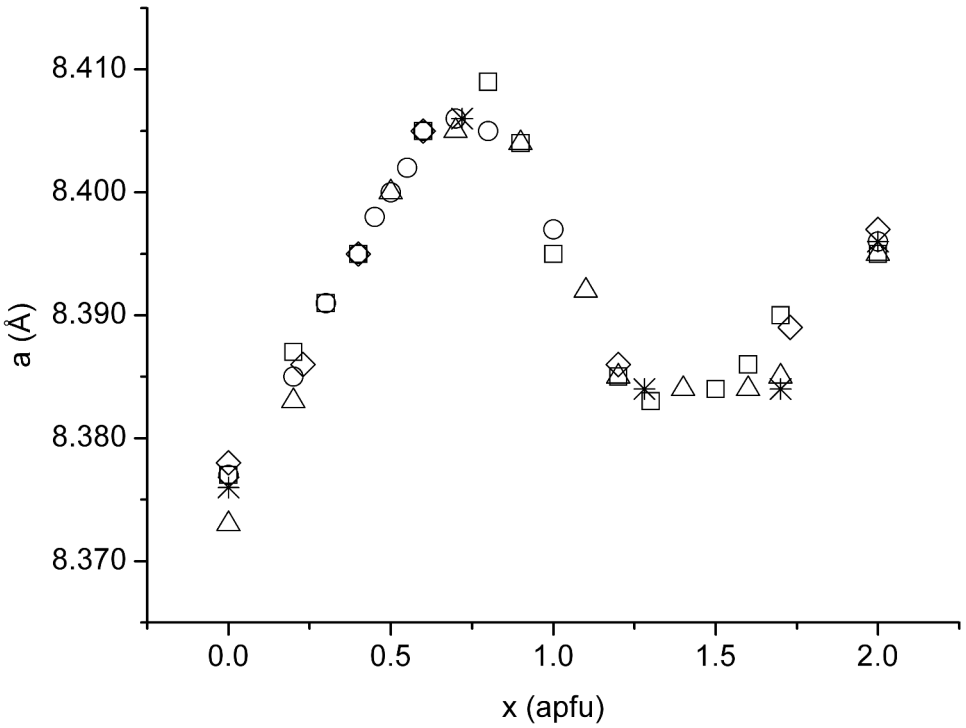

Figure 1. Variation of unit cell parameter with composition (x = Fe^{3+} = 2-Cr apfu) in the $Fe_{(1+x)}Cr_{(2-x)}O_4$ solid solution system. Data from literature: crosses = Yearian et al. (1954); circles = Francombe (1957); squares = Robbins et al. (1971); triangles = Wasilewski et al. (1975); diamonds = Gillot et al. (1976).

materials. When working with synthetic single crystals, on the contrary, the whole chemical and structural characterization can be performed on the same sample, with the advantage of greatly constraining the uncertainty of cation site distribution. This coupled chemical-structural method has been applied very successfully to study spinel order-disorder and its relationships with temperature (Andreozzi et al., 2000; Andreozzi et al., 2001a; Andreozzi and Lucchesi, 2002; Hålenius et al., 2002; Martignago et al., 2006; Bosi et al., 2007).

In order to detected the actual mineral composition, electron microprobe (EMP) is commonly used, but it has the limitation to not recognize the multiple oxidation states of transition metals. As a consequence, the Fe^{2+}/Fe^{3+} ratio is usually calculated upon mineral stoichiometry and charge balance, i.e., for spinels assuming a proportion of 3 cations to 4 anions. This approach totally ignores the possibility of non-stoichiometry, which can be due to either Fe^{3+} excess and cation vacancies in the lattice or cation excess and anion vacancies. Notably, this latter case has been addressed by Fregola et al. (2011) in this special issue. In case of non-stoichiometry, therefore, systematic errors may be very large and Fe^{2+}/Fe^{3+} ratios based on EMP results turn out to be valueless because of the wrong starting assumptions. As for example, small errors in Fe^{2+}/Fe^{3+} ratio for natural samples may produce large errors in

mantle parameters evaluation and seriously affect petrologic interpretations (Wood and Virgo, 1989; Sobolev et al., 1999; Quintiliani, 2006).

^{57}Fe Mössbauer spectroscopy (MS) is a very effective method to investigate actual iron oxidation state in minerals phases and their mineral inclusions (Wood and Virgo, 1989; McCammon et al., 1998; Sobolev et al., 1999). An important and frequent application of MS to spinels is the determination of highly accurate Fe^{2+}/Fe^{3+} ratios and attribution of Fe^{2+} and Fe^{3+} to T and M sites (e.g., Andreozzi et al., 2001b; Hålenius et al., 2002 and references therein). Fe^{2+}/Fe^{3+} ratios are obtained by measuring the absorption areas of Fe^{2+} and Fe^{3+} subspectra, which are proportional to the product of the number of absorption nuclei times the recoil-free fraction (f). The f factor is determined by lattice vibrations of the probe atoms and may suffer from temperature influence (Sawatzky et al., 1969; De Grave and Van Alboom, 1991; Eeckhout and De Grave, 2003). Moreover, the f factors for Fe^{2+} (f_2) and Fe^{3+} (f_3) are not equal at room temperature but, in spite of this, they are commonly assumed to be equal for a given phase.

In the present work, spinel single crystals belonging to region I of the chromite-magnetite join were synthesized and investigated by a combined microanalytical, diffractometric and spectroscopic approach.

Samples and Methods

Synthesis

Spinel single-crystals in the $Fe_{1+x}Cr_{2-x}O_4$ ($0 \leq x \leq 2/3$) system were synthesized by a flux-growth method in the laboratories of Rome and Stockholm. Starting materials consisted of analytical grade Fe_2O_3 and Cr_2O_3 powders, which were dehydrated and dried at 900 °C for 1 hour, before being mixed with $Na_2B_4O_7$, used as flux component. $Na_2B_4O_7$ was chosen for its low melting point (742.5 °C), the low-energy barriers to crystal growth in the borate flux (Berkes and White, 1969), and its absence of interaction with spinel compositions. Starting from the Flux/Nutrients (F/N) ratio of 3.2 used by Lenaz and Skogby (2003) for producing $FeCr_2O_4$, F/N ratio for intermediate compositions was determined by trial and error. About 2 g of starting material were thoroughly ground and mixed under acetone in an agate mortar and then transferred to a Yttrium-stabilized 10-cc Pt/Au (5%) crucible. The latter was suspended inside a vertical furnace whose heating elements guarantee a homogeneous temperature zone of 30 cm. The furnace is equipped with a multi-step temperature controller and an oxygen fugacity control system, which uses a binary gas mixture (CO_2 - H_2). The ratio CO_2/H_2 was kept constant at 58/2 and oxygen fugacity ranged from 10^{-8} to 10^{-13} bars at 1200 and 900 °C, respectively. During thermal runs, both temperature and fO_2 were monitored by sensors close to the crucible and were recorded by a computer software.

Following the procedure described by Andreozzi (1999) and Lenaz and Skogby (2003), thermal runs were started with a rather steep increment up to 1200 °C, after which the temperature was kept constant for 24 hours for complete dissolution and homogenization of the oxide mixture. Subsequently, the temperature was linearly decreased down to 900 °C with 4 °C/h cooling rate, followed by faster cooling down to ambient temperature. It was observed that the influence of cooling path was very low when appropriate F/N ratio was achieved.

Products consisted of an intergrowth of octahedral spinels and elongated, prismatic iron borate crystals embedded in minor sodium borate glass. The spinel crystals grew on the walls of the crucible, on the surface of the melt, and in the bulk mass. The products were immersed in hot, dilute hydrochloric acid for few days in order to dissolve glass and borates.

Spinel crystals were handpicked under a binocular microscope. The amount of spinel recovered from each run ranged from 80 mg to more than 1000 mg, corresponding to some hundred single crystals.

X-ray powder diffraction

To verify the sole presence of spinel phase and to calculate the unit cell parameter of the synthetic batch samples, X-ray powder diffraction (XRPD) analysis was performed. About 10 mg of crystals were handpicked, cleaned in an ultrasonic bath, and ground under acetone in an agate mortar. Data were collected by means of a SEIFERT MZ IV diffractometer covering a collection range of 15-120° 2θ angle for all samples with a collection time of 5 seconds per degree. Silicon was used as internal standard. Unit cell parameters was derived by using the LUSCRIPT software by using the strongest diffraction peaks.

Electron microprobe analysis

Electron microprobe analysis was performed in order to obtain chemical composition of synthetic spinel crystals. Chemical homogeneity was checked by analyzing different crystals of each batch, with an average of 10 spot analyses per crystal adopting a step of 10 μm from rim to core. Single crystals of different size (from 50 to 300 μm) were analyzed: they were mounted on glass slides, thinned, polished and carbon coated for electron microprobe analysis at IGAG-CNR laboratory in Rome. Spinel analyses were carried out using the Cameca/ Camebax instrument operating at an accelerating potential of 15 kV and a sample current of 15 nA, using Wavelength Dispersive System. Synthetic Fe_2O_3 and Cr_2O_3 were used as standards. Aluminum was also checked for, in order to highlight any contamination from the alumina tube, but was not detected. Raw data were reduced by PAP-type correction software provided by Cameca (Pouchou and Pichoir, 1984). Each element determination was accepted after checking that the intensity of the analyzed standard before and after each measurement was within 1.00 ± 0.01. Precision for major elements was usually within 1% of the actual amount present.

Mössbauer spectroscopy

Mössbauer spectroscopy analysis was used to obtain Fe^{3+}/Fe_{tot} ratios. Absorbers were prepared by pressing finely ground spinel samples mixed with powdered acrylic resin (Lucite) to self-supporting discs. The amount used corresponded to about 2 mg Fe/cm^2 and was well below an absorber density where thickness affects the Mössbauer results. Spectra were collected at 298 K (Room Temperature, RT) using a conventional spectrometer system operating in constant acceleration mode with a ^{57}Co source in rhodium matrix. Spectral data for the velocity range -4 to +4 mm/s were recorded in a multichannel analyzer using 512 channels. After velocity calibration with a high purity α-iron foil spectra, the raw data were folded in 256 channels. The spectra were fitted using the Recoil 1.04 (Lagarec and Rancourt, 1998) fitting program and assuming symmetrical Lorentian peak shapes. The best fits were evaluated by reduced χ^2, and uncertainties were calculated using the covariance matrix. Uncertainty is estimated about ±0.02 mm/s for isomer shift (δ), quadrupole splitting (ΔE_Q) and peak width (Γ). Spectral areas for Fe^{2+} and Fe^{3+} were corrected with *f* factors calculated by De Grave and Van Alboom (1991) for RT conditions (average values for Fe-bearing spinel compositional range: $f_2 = 0.687$ and $f_3 = 0.887$). Uncertainty associated with doublet areas is estimated to be less than ± 3%.

Results and Discussion

Synthesis products

A total of 23 experimental runs were

performed with various starting compositions and F/N ratios. Each thermal run produced single crystals of different quality and yield. Crystals quality was tested by observations at both optical microscope and Scanning Electron Microscope (SEM). For each batch, largely variable crystal sizes were observed (from few μm to several hundred μm). Nevertheless, for each batch a main crystal size was empirically estimated, that is a combination between size and frequency of occurrence.

Spinel single crystals appear as black, regular or truncated octahedra, with main size ranging from 50 to 300 μm and total yield from 0.01 to 1 g (Figure 2 and Table 1). The iron-poor compositions were more easily synthesized. For batches FeCr100, FeCr90, FeCr80 and FeCr70, products of sufficient yield and quality were obtained with a single run so that thermal runs with different F/N ratio were not necessary. In fact, an influence of F/N ratio on crystal yield and quality was observed. The yield decreased at increasing F/N ratios, as shown for example by FeCr40 runs, but it was noted that in some cases large yield corresponded to small and poor quality crystals (Table 1). A relatively high F/N ratio always promoted good quality products for all compositions. However, a high F/N ratio gave a crystal composition different with respect to that of the starting oxide mixture. As a result, a general shift towards the Cr-rich compositions was observed.

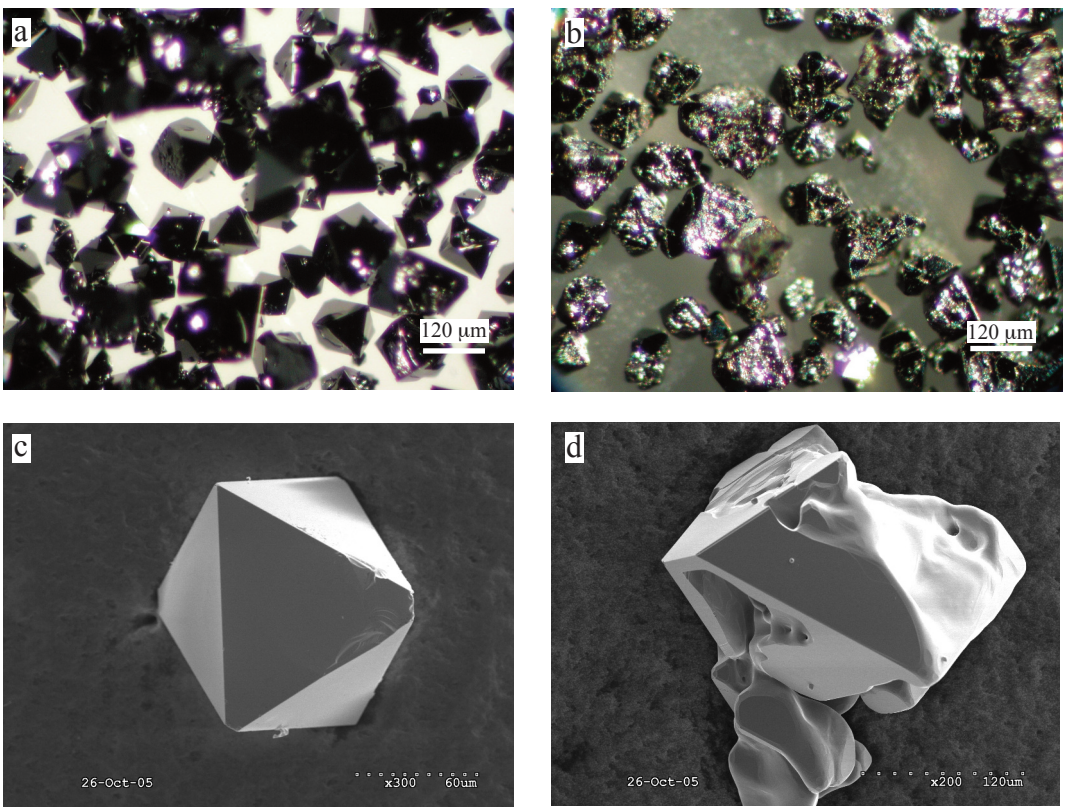

Figure 2. Optical and SEM pictures of selected synthetic spinel crystals: a, c) good quality; b, d) poor quality.

Table 1. Results of synthesis runs in the Fe-Cr spinel system.

Run	Sample	F/N	main size (μm)	yield (g)
1	FeCr100	3.2	300	~1.00
2	FeCr90	2.9	300	~1.00
3	FeCr80	2.5	300	~1.00
4	FeCr70	2.1	300	~1.00
5	FeCr60A	1.8	300	~1.00
6	FeCr60B	2.3	100	0.15
7	FeCr50A	1.5	150	~1.00
8	FeCr50B	1.7	150	0.46
9	FeCr50C	1.9	150	0.49
10	FeCr50D	2.1	150	0.56
11	FeCr50E	2.5	100	0.09
12	FeCr40A	1.2	50	~1.00
13	FeCr40B	1.55	80	0.63
14	FeCr40C	1.7	100	0.45
15	FeCr40D	2.1	100	0.16
16	FeCr30A	1.8	50	0.01
17	FeCr30B	2.0	200	0.15
18	FeCr30C	2.2	200	0.09
19	FeCr20A	2.2	50	0.15
20	FeCr20B	2.4	80	0.21
21	FeCr20C	2.2	100	0.09
22	FeCr20D	2.4	100	0.22
23	FeCr10A	2.2	100	0.08

XRPD and EMP data

The absence of extra phases other than spinel was checked in every batch by XRPD analysis, which was used also to obtain a representative value of unit cell parameter for every batch (Table 2). Chemical data are reported as the average value of several point analyses collected on various crystals of the same batch (Table 2). Mean chemical composition is expressed in terms of the $Fe_{1+x}Cr_{2-x}O_4$ system (x = Fe^{3+} = 2-Cr apfu), chosen to represent the chromite-magnetite series by several authors (e.g. Levinstein et al., 1972). The crystals examined cover the region I of the series, with x ranging from 0.00 to 0.67 apfu. The percentage of magnetite was estimated starting from the Cr content, considering that it varies linearly from chromite (2 apfu) to magnetite (zero apfu).

In most cases, a chemical heterogeneity was observed among different crystals of the same batch, as quantified by large standard deviations of Cr contents (Table 2). Within single crystals, small ones are more homogeneous than bigger ones (Figure 3). This large inter- and intracrystalline heterogeneity could be explained by growth of many generations of crystals with different size and composition during the same thermal run.

Unit cell parameter of our crystals increases linearly with chemical composition (Figure 4).

Table 2. Cell parameter and mean composition of synthetic spinel samples belonging to the chromite-magnetite series.

Batch	FeCr100	FeCr90	FeCr80	FeCr70	FeCr60B	FeCr60A	FeCr50E	FeCr30C	FeCr50C	FeCr50D	FeCr10A
a (Å)	8.3781(2)	8.3798(2)	8.3804(5)	8.3847(4)	8.3962(5)	8.3882(2)	8.3884(5)	8.3898(5)	8.3936(4)	8.3906(12)	8.3990(8)
Cr_2O_3 (wt.%)	67.7(3)	67.5(2)	65.7(5)	65(1)	61(2)	60(2)	58.8(7)	57(1)	55(1)	57(1)	53(7)
FeO_{tot} (wt.%)	31.9(2)	33.1(1)	34.8(4)	35(1)	39(2)	39(1)	39.8(8)	38.9(5)	39(1)	42(1)	44(7)
Total	99.6	100.6	100.5	100	100	99	98.6	95.9	94	99	97
Cr (apfu)	2.00	1.97	1.92	1.89	1.79	1.77	1.75	1.74	1.69	1.68	1.58
Fe^{3+} (apfu)	0.00	0.03	0.08	0.11	0.21	0.23	0.25	0.26	0.31	0.32	0.42
Fe^{2+} (apfu)	1.00	1.00	1.00	1.00	1.00	1.00	1.00	1.00	1.00	1.00	1.00
Total	3.00	3.00	3.00	3.00	3.00	3.00	3.00	3.00	3.00	3.00	3.00
Fe^{3+}/Fe_{tot} (%)	0	3	7	10	17	19	20	20	23	24	30
Magnetite (%)	0	1	4	6	11	12	13	13	15	16	21

Batch	FeCr50A	FeCr20A	FeCr50B	FeCr40D	FeCr20C	FeCr20B	FeCr20D	FeCr30B	FeCr40C	FeCr40A
a (Å)	8.3983(7)	8.3948(2)	8.3957(6)	8.3906(5)	8.3942(5)	8.3937(5)	8.4040(11)	8.3935(5)	8.3946(4)	8.3994(5)
Cr_2O_3 (wt.%)	53(1)	52(2)	52.1(4)	49.2(6)	51(3)	51(2)	51(4)	48(1)	49(1)	44(2)
FeO_{to}t (wt.%)	46.1(9)	45(3)	46.2(2)	44.3(9)	46(3)	46(1)	47(4)	45(1)	49(1)	53(3)
Total	98.7	97	98.3	93.5	97	97	98	93	98	97
Cr (apfu)	1.56	1.56	1.55	1.54	1.53	1.52	1.52	1.51	1.46	1.33
Fe^{3+} (apfu)	0.44	0.44	0.45	0.46	0.47	0.48	0.48	0.49	0.54	0.67
Fe^{2+} (apfu)	1.00	1.00	1.00	1.00	1.00	1.00	1.00	1.00	1.00	1.00
Total	3.00	3.00	3.00	3.00	3.00	3.00	3.00	3.00	3.00	3.00
Fe^{3+}/Fe_{tot} (%)	31	31	31	32	32	32	32	33	35	40
Magnetite (%)	22	22	23	23	23	24	24	25	27	33

Notes: Chemical data are the average of 20-40 EMP analyses collected on various crystals of the same batch. Number of ions on the basis of spinel stoichiometry (3 cations per 4 anions). Estimated standard deviation (±1σ) in brackets.

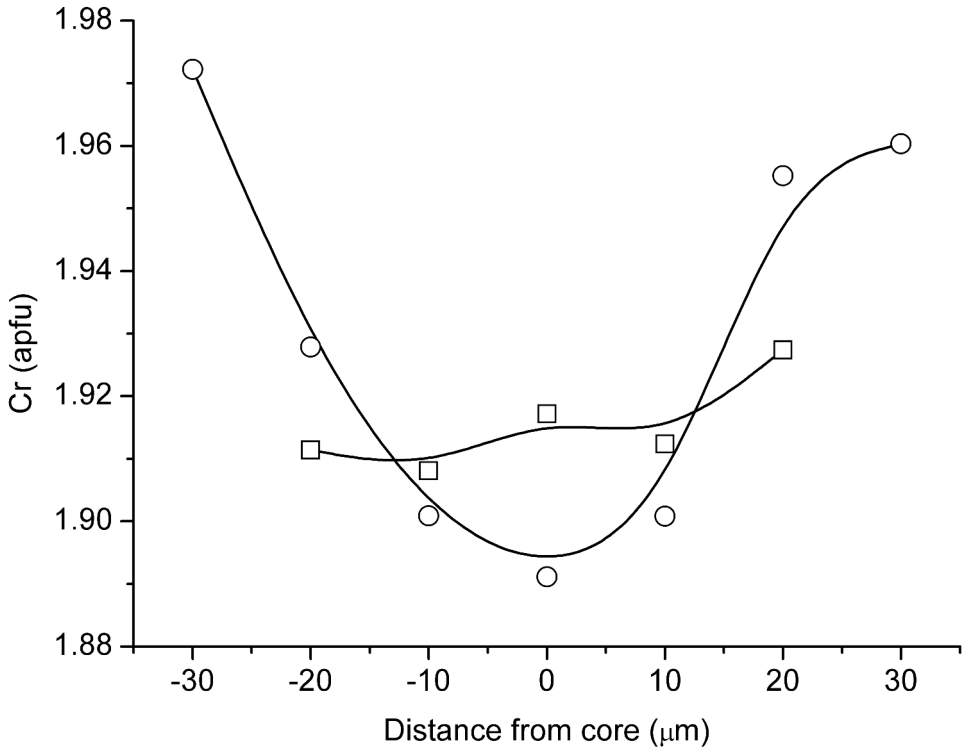

Figure 3. Comparison between Cr content of two selected crystals from FeCr80 run. Circles = large crystal; squares = small crystal. A step of 10 μm was adopted during EMP spot analysis.

In the same diagram literature data of spinels belonging to the Cr-rich portion of the series are added for comparison and a general agreement may be observed, with the largest deviation shown by the chromite end member of Wasilewski et al. (1975).

^{57}Fe Mössbauer spectroscopy data

All Mössbauer spectra are dominated by an absorption signal centered at ca. 0.9 mm/s which, according to the existing literature, was assigned to Fe^{2+} in the tetrahedrally coordinated T site (Robbins et al., 1971; Osborne et al., 1981; 1984). For the chromite end member the Fe^{2+} absorption is merely a singlet (Figure 5), but with increasing magnetite component it splits into a doublet. The evolution from singlet to doublet may be ascribed to the next-nearest-neighbor effect, i.e., non-spherical cation distribution in the second coordination sphere of the T site, that is made of 12 M sites (Waerenborgh et al., 1990; 1994). With the exception of chromite end member, FeCr100, all samples show an additional absorption band in the spectral region between zero and 1 mm/s, commonly assigned to Fe^{3+} (Figure 6). In all cases, there was no evidence of an absorption sextet in the outer part of the spectra, so that the presence of magnetic phases was excluded.

Mössbauer spectra were tested with several fitting models, looking for the best solution with the least number of signals and constraints.

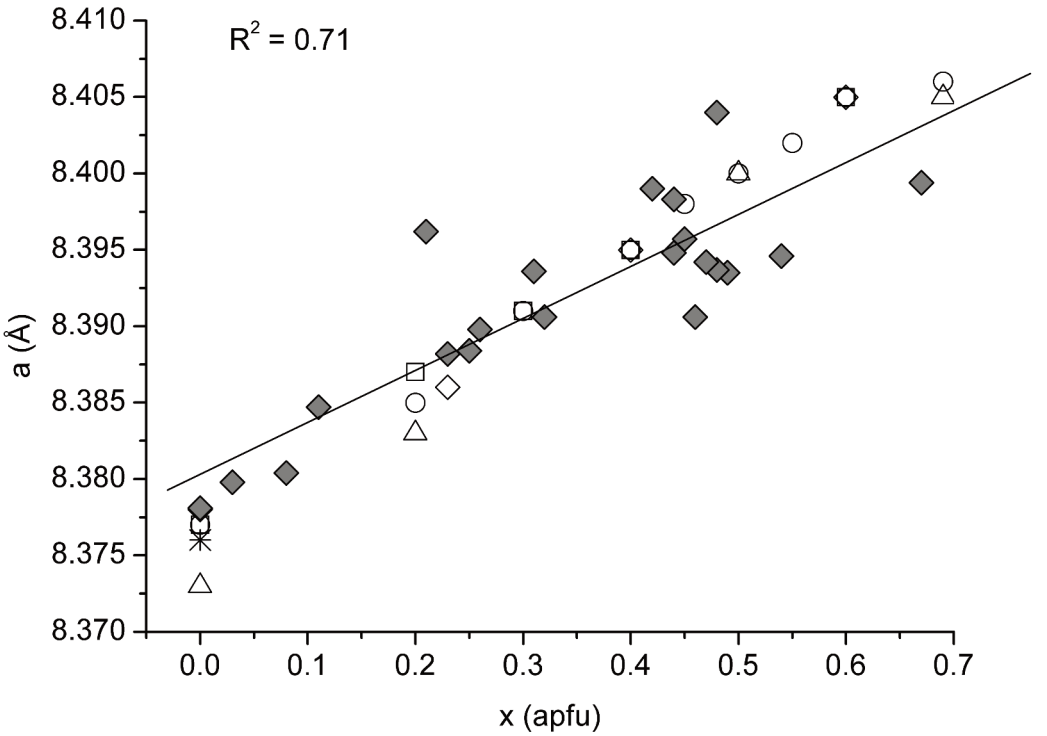

Figure 4. Variation of unit cell parameter with composition (x = Fe^{3+} = 2-Cr apfu) in synthetic crystals belonging to the Cr-rich portion of the chromite-magnetite series. Full diamonds = studied samples. Solid line = best fit to studied samples. Asterisks = Yearian et al. (1954); circles = Francombe (1957); squares = Robbins et al. (1971); triangles = Wasilewski et al. (1975); open diamonds = Gillot et al. (1976). Cell parameter estimated uncertainties are smaller than symbol dimensions.

Spectrum of the sample FeCr100 was resolved, as expected, by a singlet ($1Fe^{2+}$) and any further contribution was systematically rejected. For the other samples, starting from a one-doublet model and tentatively adding components, an almost satisfactory fit was obtained with two-doublets model ($1Fe^{2+}$ + $1Fe^{3+}$). The attempt to use a three-doublets model was generally successful and improved the goodness of fitting parameters. The third doublet, though always minor, showed δ value intermediate between those of Fe^{2+} and Fe^{3+} and was attributed to the so-called $Fe^{2.5+}$ produced by the electron hopping. In conclusion, best results were obtained with a three-doublets model ($1Fe^{2+}$ + $1Fe^{3+}$ + $1Fe^{2.5+}$) for all samples but FeCr100.

Refined hyperfine parameters together with corrected absorption areas of all samples are listed in Table 3. Fe^{3+}/Fe_{tot} ratios obtained from Mössbauer spectroscopy are comparable (within experimental uncertainties) with those calculated following stoichiometric criteria, and linearly correlated with nominal composition, that is with increasing magnetite content (Figure 7).

In contrast with most of the literature studies, spectroscopic analysis revealed the presence of electron charge delocalization (that is $Fe^{2.5+}$), wich was unexpected in our Fe^{3+}-poor samples

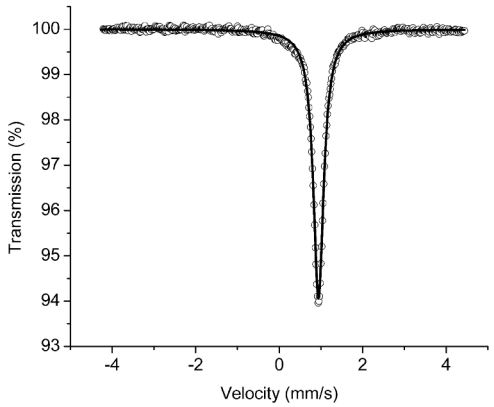

Figure 5. RT ^{57}Fe Mössbauer spectrum of FeCr100 sample: fit with one-doublet model (Fe^{2+}). Circles = experimental spectrum; black line = calculated spectrum.

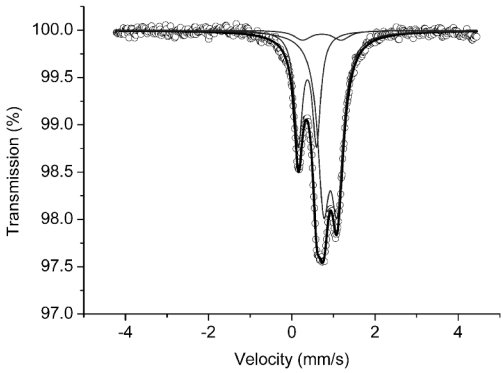

Figure 6. RT ^{57}Fe Mössbauer spectrum of FeCr10 sample: fit with three-doublets model (Fe^{2+}, Fe^{3+}, $Fe^{2.5+}$). Circles = experimental spectrum; heavy black line = calculated spectrum.

belonging to the region I of the series. The $Fe^{2.5+}/Fe_{tot}$ absorption area ranges between 1% and 6% and approximately follows the magnetite content (Table 3). Actually, the contents observed are somewhat questionable since they are close to the detection limit (at least for the lowest values), but the reality of the third doublet, unexpected in the region I of the series, has been further confirmed by structural study of selected crystals (Andreozzi et al., 2007; Andreozzi and Quintiliani, work in progress).

A solid state reaction able to account for the observed behavior could be spinodal decomposition forming chromite-rich and magnetite-rich domains which are critically small to be detected, similar to what observed sometimes in natural and synthetic samples (Golla-Schindler et al., 2005; Della Giusta et al., 2011). However, such a decomposition is very unlikely in our case since thermal runs were rapidly cooled from temperatures well above the immiscibility gap for chromite-magnetite series. In these conditions, a single phase should be quenched in, and this is supported by previous studies on crystals produced with the same process (Andreozzi et al., 2001; Lenaz et al., 2004). Moreover, the presence of magnetite was definitely excluded by Mössbauer spectroscopy analysis, as magnetic sextets were not detected in the spectra. An alternative mechanism accounting for the occurrence of electron delocalization even in Cr-rich compositions was suggested by Nell and Wood (1991) based on electrical measurements. They pointed out that in the structure of Cr-rich compositions there are few Fe^{2+} ions in octahedral coordination (due to inversion) surrounded by Cr ions as next-nearest neighbors. Given this scenario, they concluded that the activation energy measured for electrical conduction in Cr-rich compositions may represent electron hopping between Fe^{2+} and Fe^{3+} via Cr. This mechanism would explain the presence of small but actual content of $Fe^{2.5+}$ in the samples studied in this work.

Acknowledgments

This work benefited from the precious suggestions and the active support of S. Lucchesi, to whom the authors are indebted for his life example and ethics. Sincere thanks are also due to G. Graziani for the

Table 3. ^{57}Fe Mössbauer hyperfine parameters at RT (298 K) of synthetic spinel samples belonging to the chromite-magnetite series.

Batch	δ (mm/s)	ΔEQ (mm/s)	Γ (mm/s)	A (%)	Species	χ^2	Fe^{3+}/Fe_{tot} (%)	Fe^{3+}/Fe_{tot} corr (%)
FeCr100	0.93	0.00	0.28	100	Fe^{2+}	0.5	0	0
FeCr90	0.93	0.08	0.32	93	Fe^{2+}	1.0	7	6
	0.41	0.50	0.46	6	Fe^{3+}			
	0.57	0.91	0.20	1	$Fe^{2.5+}$			
FeCr80	0.93	0.11	0.26	90	Fe^{2+}	0.4	9	7
	0.40	0.54	0.32	8	Fe^{3+}			
	0.65	0.22	0.20	2	$Fe^{2.5+}$			
FeCr70	0.93	0.16	0.28	86	Fe^{2+}	0.4	14	11
	0.38	0.46	0.26	13	Fe^{3+}			
	0.65	0.22	0.20	1	$Fe^{2.5+}$			
FeCr60B	0.93	0.19	0.30	84	Fe^{2+}	0.5	16	13
	0.36	0.46	0.22	15	Fe^{3+}			
	0.60	0.73	0.20	1	$Fe^{2.5+}$			
FeCr 60A	0.93	0.22	0.32	79	Fe^{2+}	0.7	20	16
	0.37	0.45	0.24	19	Fe^{3+}			
	0.68	0.90	0.20	2	$Fe^{2.5+}$			
FeCr50E	0.93	0.22	0.30	79	Fe^{2+}	0.7	21	17
	0.37	0.45	0.22	20	Fe^{3+}			
	0.68	0.88	0.20	1	$Fe^{2.5+}$			
FeCr30C	0.92	0.27	0.32	72	Fe^{2+}	0.4	27	22
	0.36	0.44	0.22	26	Fe^{3+}			
	0.69	0.95	0.20	2	$Fe^{2.5+}$			
FeCr50C	0.92	0.26	0.32	75	Fe^{2+}	1.0	24	20
	0.36	0.45	0.20	23	Fe^{3+}			
	0.68	0.92	0.20	2	$Fe^{2.5+}$			
FeCr50D	0.92	0.24	0.30	76	Fe^{2+}	0.5	23	19
	0.37	0.45	0.22	22	Fe^{3+}			
	0.68	0.92	0.20	2	$Fe^{2.5+}$			
FeCr10A	0.92	0.32	0.34	63	Fe^{2+}	0.4	34	29
	0.37	0.43	0.22	31	Fe^{3+}			
	0.72	0.92	0.48	6	$Fe^{2.5+}$			
FeCr50A	0.92	0.29	0.30	70	Fe^{2+}	0.6	29	24
	0.36	0.44	0.20	28	Fe^{3+}			
	0.71	0.94	0.20	2	$Fe^{2.5+}$			

Table 3. ...continued

Batch	δ (mm/s)	ΔEQ (mm/s)	Γ (mm/s)	A (%)	Species	χ^2	Fe^{3+}/Fe_{tot} (%)	Fe^{3+}/Fe_{tot} corr (%)
FeCr20A	0.92	0.32	0.34	66	Fe^{2+}	0.6	33	28
	0.37	0.43	0.24	32	Fe^{3+}			
	0.64	0.84	0.20	2	$Fe^{2.5+}$			
FeCr50B	0.92	0.27	0.34	71	Fe^{2+}	0.8	28	23
	0.36	0.45	0.22	26	Fe^{3+}			
	0.70	0.91	0.20	3	$Fe^{2.5+}$			
FeCr40D	0.93	0.29	0.32	68	Fe^{2+}	0.5	31	26
	0.39	0.45	0.22	30	Fe^{3+}			
	0.77	0.50	0.20	2	$Fe^{2.5+}$			
FeCr20C	0.93	0.30	0.36	65	Fe^{2+}	0.6	34	29
	0.37	0.43	0.26	33	Fe^{3+}			
	0.69	1.96	0.20	2	$Fe^{2.5+}$			
FeCr20B	0.93	0.28	0.32	69	Fe^{2+}	0.4	30	25
	0.37	0.44	0.22	28	Fe^{3+}			
	0.72	0.90	0.20	3	$Fe^{2.5+}$			
FeCr20D	0.93	0.35	0.36	60	Fe^{2+}	2.9	38	32
	0.37	0.42	0.26	36	Fe^{3+}			
	0.64	1.80	0.46	4	$Fe^{2.5+}$			
FeCr30B	0.92	0.31	0.32	67	Fe^{2+}	0.4	32	27
	0.36	0.43	0.22	31	Fe^{3+}			
	0.71	0.98	0.20	2	$Fe^{2.5+}$			
FeCr40C	0.94	0.30	0.30	62	Fe^{2+}	0.4	36	30
	0.38	0.45	0.22	33	Fe^{3+}			
	0.77	0.47	0.20	5	$Fe^{2.5+}$			
FeCr40A	0.91	0.37	0.41	58	Fe^{2+}	0.9	41	35
	0.37	0.41	0.32	39	Fe^{3+}			
	0.66	1.95	0.42	3	$Fe^{2.5+}$			

Notes: δ = isomer shift (with respect to α-iron); ΔEQ = quadrupole splitting; Γ = full width at half maximum; A = area. Estimated uncertainties (σ) are about 0.02 mm/s for δ, ΔEQ and Γ, and no less than 3% for RT spectral areas.

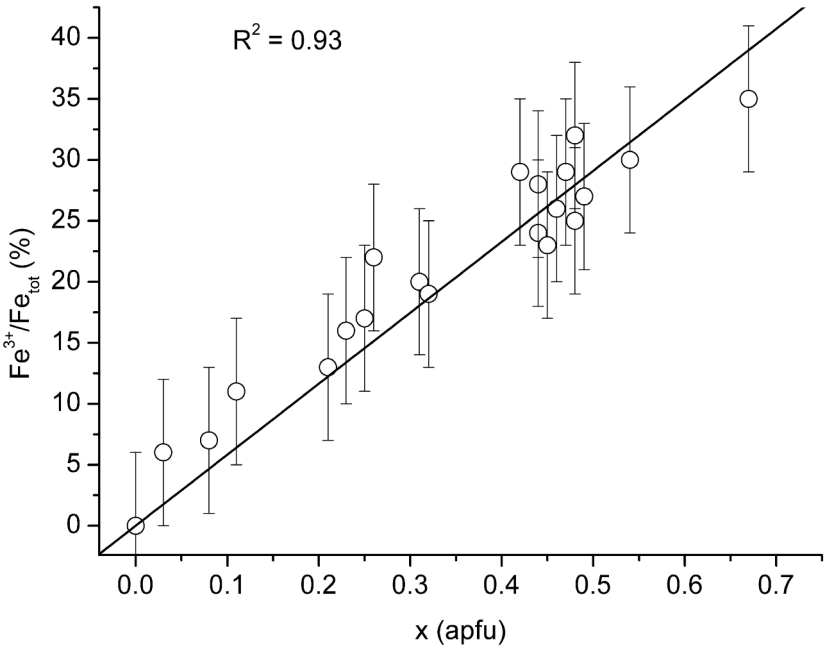

Figure 7. Variation of measured Fe^{3+}/Fe_{tot} ratios with composition (x = Fe^{3+} = 2-Cr apfu) in synthetic crystals belonging to the Cr-rich portion of the chromite-magnetite series. Error bars = ±2σ. Solid line = best fit.

synthesis laboratory setup and to A. Della Giusta for constructive revision. M. Serracino and S. Stellino kindly assisted during EMP and XRPD data collection, respectively. Financial support from Synthesis European Programme at NRM (Swedish Natural Science Museum of Stockholm) and the italian PRIN 2008 "SPIN GEO-TECH" are gratefully aknowledged.

References

Andreozzi G.B. (1999) - Synthetic spinels in the (Mg, Fe^{2+}, Zn)(Al, Fe^{3+})$_2O_4$ system: I. Flux growth of single crystals. *Periodico di Mineralogia*, 68(1), 43-51.

Andreozzi G.B., Princivalle F., Skogby H. and Della Giusta A. (2000) - Cation ordering and structural variations with temperature in $MgAl_2O_4$ spinel: an X-ray single crystal study. *American Mineralogist*, 85, 1164-1171.

Andreozzi G.B., Bosi F. and Garramone F. (2001a) - Synthetic spinels in the (Mg, Fe^{2+}, Zn)(Al, Fe^{3+})$_2O_4$ system: II. Preliminary chemical and structural data of hercynite and magnesioferrite samples. *Periodico di Mineralogia*, 70, 193-204.

Andreozzi G.B., Hålenius U. and Skogby H. (2001b) - Spectroscopic active $^{IV}Fe^{3+}$-$^{VI}Fe^{3+}$ clusters in spinel-magnesioferrite solid solution crystals: a potential monitor for ordering in oxide spinels. *Physics and Chemistry of Minerals*, 28, 435-444.

Andreozzi G.B. and Lucchesi S. (2002) - Intersite distribution of Fe^{2+} and Mg in the spinel (sensu-stricto)-hercynite series by single-crystal X-ray diffraction. *American Mineralogist*, 87, 113-1120.

Andreozzi G.B., Quintiliani S. and Lucchesi S. (2007) - Experimental approach to chromite-magnetite solid solution: Synthesis, characterization (XRD-SREF, EMPA, MS) and cation distribution of $Fe_{1+x}Cr_{2-x}O_4$ ($0 < x < 0.5$) spinel single crystals. Frontiers in Mineral Sciences 2007, Cambridge (UK), 26-28 June 2007.

Ballhaus C., Berry R.F. and Green D.H. (1991) - High pressure experimental calibration of the olivine-orthopyroxene-spinel oxygen geobarometer: implications for the oxidation state of the upper mantle. *Contributions to Mineralogy and Petrology*, 107, 27-40.

Barrero C.A., Morales A.L., Restrepo J., Pérez G., Tobòn J., Mazo-Zuluaga J., Jaramillo F., Escobar D.M., Arroyave C.E., Vandenberghe R.E. and Greneche J.-M. (2001) - Synthesis of magnetite in presence of Cu^{2+} or Cr^{3+}. *Hyperfine Interactions*, 134, 141-152.

Berkes J.S. and White W.B. (1969) - Structural characteristic of alkali borate flux liquids. *Journal of Crystal Growth*, 6, 29-42.

Bosi F., Hålenius U., Andreozzi G.B., Skogby H. and Lucchesi S. (2007) - Structural refinement and crystal chemistry of Mn-doped spinels: A case for tetrahedrally coordinated Mn^{3+} in an oxygen-based structure. *American Mineralogist*, 92, 27-33.

Daniels J.M. and Rosencwaig A. (1969) - Mössbauer spectroscopy of stoichiometric and non-stoichiometric magnetite. *Journal of Physics and Chemistry of Solids*, 30, 1561-1571.

De Grave E. and Van Alboom A. (1991) - Evaluation of ferrous and ferric Mössbauer fraction. *Physics and Chemistry of Minerals*, 18, 337-342.

Derbyshire W.D. and Yearnian H.J. (1958) - X-Ray diffraction and magnetic measurements of the Fe-Cr spinels. *Physical Review*, 112(5), 1603-1607.

Della Giusta A., Carbonin S. and Russo U. (2011) - Chromite to magnetite transformation: compositional variations and cation distutions (southern Aosta Valley, Western Alps, Italy). *Periodico di Mineralogia*, 80(1), 1-18.

Dick H.J.B. and Bullen T. (1984) - Chromian spinel as a petrogenetic indicator in abyssal and alpine-type peridotites and spatially associated lavas. *Contributions to Mineralogy and Petrology*, 86, 54-76.

Eeckhout S.G. and De Grave E. (2003) - Evaluation of ferrous and ferric Mössbauer fraction. Part II. *Physics and Chemistry of Minerals*, 30, 142-146.

Fabriès J. (1979) - Spinel-olivine geothermometry in peridotites from ultramafic complexes. *Contributions to Mineralogy and Petrology*, 69, 329-336.

Fierro G., Lo Jacono M., Dragone R., Ferraris G., Andreozzi G.B. and Graziani G. (2005) - Fe-Zn manganite spinels and their carbonate precursors: preparation, characterization and catalytic activity. *Applied Catalysis B: Environmental,* 57, 153-165

Francombe M.H. (1957) - Lattice changes in spinel-type iron chromites. *Journal of Physics and Chemistry of Solids*, 3, 37-43.

Fregola R.A., Bosi F. and Skogby H. (2011) - A first report on anion vacancies in a defect $MgAl_2O_4$ natural spinel. *Periodico di Mineralogia*, 80(1), 27-38.

Gillot B., Ferriot J.F., Dupré G. and Rousset A. (1976) - Study of the oxidation kinetics of finely-divided magnetites. II- Influence of chromium substitution. *Material Research Bulletin*, 11, 843-850.

Golla-Schindler U., O'Neill H.St.C. and Putnis A. (2005) - Direct observation of spinodal decomposition in the magnetite-hercynite system by susceptibility measurements and transmission electron microscopy. *American Mineralogist*, 90, 1278-1283.

Hålenius U., Skogby H. and Andreozzi G.B. (2002) - Influence of cation distribution on the optical absorption spectra of Fe^{3+}-bearing spinel s.s.-hercynite crystals: evidence for electron transition in $^{VI}Fe^{2+}$-$^{VI}Fe^{3+}$clusters. *Physics and Chemistry of Minerals*, 29, 319-330.

Ishikawa T., Nakazaki H., Yasukawa A., Kandori K. and Seto M. (1999) - Influences of Co^{2+}, Cu^{2+} and Cr^{3+} ions on the formation of magnetite. *Corrosion Science*, 41, 1665-1680.

Kose K. and Lida S. (1984) - Interacting phase transition in the $Fe_{1+x}Cr_{2-x}O_4$ ($0 \leq x \leq 0.4$). *Journal of Applied Physics*, 55, 2321-2323.

Lagarec K. and Rancourt D.G. (1998) - RECOIL. Mössbauer spectral analysis software for Windows, version 1.0. Department of Physics, University of Ottawa, Canada.

Lenaz D. and Skogby H. (2003) - Flux growth of single crystal spinels in the $(Mg,Fe^{2+})(Cr,Fe^{3+})_2O_4$ system. *Periodico di Mineralogia*, 72, 69-78.

Lenaz D., Skogby H., Princivalle F. and Hålenius U. (2004) - Structural changes and valence states in the $MgCr_2O_4$-$FeCr_2O_4$ solid solution series. *Physics and Chemistry of Minerals*, 31, 633-642.

Levinstein H.J., Robbins M. and Capio C. (1972) - A crystallographic study of the system $FeCr_2O_4$ -Fe_3O_4 ($Fe^{2+}Fe^{3+}{}_xCr_{2-x}O_4$). *Materials Research Bulletin*, 7, 27-34.

Marshall C.P. and Dollase W.A. (1984) - Cation arrangement in iron-zinc-chromium spinel oxides. *American Mineralogist*, 69, 928-936.

Martignago F., Andreozzi G.B. and Dal Negro A. (2006) - Thermodynamics and kinetics of cation ordering in natural and synthetic $Mg(Al,Fe^{3+})_2O_4$ spinels from in situ high-temperature X-ray diffraction. *American Mineralogist*, 91, 306-312.

McCammon C.A., Chinn I.L., Gurney J.J. and McCallum M.E. (1998) - Ferric iron content of mineral inclusions in diamonds from George Creek, Colorado determined using Mössbauer spectroscopy. *Contributions to Mineralogy and Petrology*, 133, 30-37.

Nell J. and Wood B.J. (1991) - High-temperature electrical measurements and thermodynamic properties of Fe_3O_4-$FeCr_2O_4$-$MgCr_2O_4$-$FeAl_2O_4$ spinels. *American Mineralogist*, 76, 405-426.

O'Neill H.St.C. and Wall V.J. (1987) - The olivine-orthopiroxene-spinel oxygen geobarometer, the nickel precipitation curve, and the oxygen fugacity of the Earth upper mantle. *Journal of Petrology*, 28, 1169-1191.

Ok H.N., San Pan L. and Evans B.J. (1978) - Fe^{57} Mössbauer study of chromium-doped magnetite, $Fe_{3-x}Cr_xO_4$ ($0 \leq x \leq 0.5$) above the Verwey transition. *Physical Review* B, 17, 85-90.

Osborne M.D., Fleet M.E. and Bancroft G.M. (1981) - Fe^{+2}-Fe^{+3} ordering in chromite and Cr-bearing spinels. *Contributions to Mineralogy and Petrology*, 77, 251-255.

Osborne M.D., Fleet M.E. and Bancroft G.M. (1984) - Next-nearest neighbor effects in the Mössbauer spectra of (Cr,Al) spinels. *Journal of Solid State Chemistry*, 53, 174-183.

Petric A. and Jacob K.T. (1982) - Thermodynamic Properties of Fe_3O_4-FeV_2O_4 and Fe_3O_4-$FeCr_2O_4$ Spinel Solid Solution. *Journal of American Ceramic Society*, 65(2), 117-123.

Pouchou J.L. and Pichoir F. (1984) - A new model for quantitative X-ray micro-analysis. I. Application to the analysis of homogeneous samples. *La Recherche Aérospatiale*, 3, 13-36.

Quintiliani M., Andreozzi G.B. and Graziani G. (2006) - Fe^{2+} and Fe^{3+} quantification by different approaches and f_{O2} estimation for Albanian Cr-spinels. *American Mineralogist*, 91, 907-916.

Robbins M., Wertheim G.K., Sherwood R.C. and Buchanan D.N.E. (1971) - Magnetic properties and site distribution in the system $FeCr_2O_4$ Fe_3O_4 (Fe^{2+} $Cr_{2-x}Fe^{3+}{}_xO_4$). *Journal of Physics and Chemistry of Solids*, 32, 717-729.

Roeder P.L., Campbell I.H. and Jamieson H. (1979) - A re-evaluation of the olivine-spinel geothermometer. *Contributions to Mineralogy and Petrology*, 68, 325-334.

Sack R.O. (1982) - Spinels as petrogenetic indicator: Activity-composition relations at low pressures. *Contributions to Mineralogy and Petrology*, 79, 169-182.

Sawatzky G.A., Van Der Woude F. and Morrish A.H. (1969) - Recoilness-fraction ratio for ^{57}Fe in octahedral and tetrahedral sites of a spinel and a garnet. *Physical Reviews*, 183(2), 383-386.

Shukla S.J., Jadhav K.M., Bichile G.K. (1999) - Influence of Mg^{2+} substitution on magnetic properties of Co-Fe-Cr-O spinel ferrite system. *Journal of Magnetism and Magnetic Materials,* 195, 692-698.

Sobolev V.N., McCammon C.A., Taylor L.A., Snyder G.A. and Sobolev N.V. (1999) - Precise Mössbauer milliprobe determination of ferric iron in rock-forming minerals and limitations of electron microprobe analysis. *American Mineralogist*, 84, 78-85.

Verwey E.J.W., Haayman P.H. and Romeijn F.C. (1947) - Physical properties and cation arrangement of oxides with spinel structures. II. Electronic conductivity. *Journal of Chemical Physics*, 15, 181-187.

Viart N., Pourroy G., Grenèche J.M., Niznansky D. and Hommet J. (2000) - Microstructural and magnetic properties of Fe/Cr-substituted ferrite composites. *European Physical Journal of Applied Physics*, 12, 37-46.

Waerenborgh J.C., Annersten H., Ericsson T., Figuereido M.O. and Cabral J.M.P. (1990) - A Mössbauer study of natural gahnite spinels showing strongly temperature dependent quadrupole splitting distributions. *European Journal of Mineralogy*, 2, 267-271.

Waerenborgh J.C., Figuereido M.O. and Cabral J.M.P. (1994) - Temperature and composition dependence of the cation distribution in $ZnFe_yAl_{2-y}O_4$ ($0 < y \leq 2$) spinels. *Journal of Solid State Chemistry*, 111(2), 300-309.

Wasilewski P., Virgo D., Ulmer G.C. and Schwerer F.C. (1975) - Magnetochemical characterization of $Fe(Fe_xCr_{2-x})O_4$ spinels. *Geochimica et Cosmochimica Acta*, 39, 889-902.

Wood B.J. and Virgo D. (1989) - Upper mantle oxidation state: Ferric iron contents of lherzolite spinels by ^{57}Fe Mössbauer spectroscopy and resultant oxygen

fugacities. *Geochimica et Cosmochimica Acta*, 53, 1277-1291.

Yearian H.J., Kortright J.M. and Langenheim R.H. (1954) - Lattice parameters of the $FeFe_{2-x}Cr_xO_4$ spinel system. *Journal of Chemical Physics*, 22(7), 1196-1198.

Yunus S.M., Yamauchi H., Zakaria A.K.M., Igawa N., Hoshikawa A. and Ishii Y. (2008) - Cation distribution and crystallographic characterization of the quaternary spinel system $Mg_xCo_{1-x}CrxFe_{2-x}O_4$. *Journal of Alloys and Compounds,* 454, 10-15.

Ziemniak S.E. and Castelli A.C. (2003) - Immiscibility in the Fe_3O_4-$FeCr_2O_4$ spinel binary. *Journal of Physics and Chemistry of Solids*, 64, 2081-2091.

Submitted, October 2010 - Accepted, January 2011